# DISCRETE RANDOM STRUCTURES: RANDOM DOMINO TILINGS (PRELIMINIARY VERSION)

### SUNIL CHHITA

### 1. Lecture 1

1.1. Motivation. Random tiling models serve as toy models for two dimensional statistical mechanical models. One of their attractions is that they are exactly solvable, meaning that the partition function can be computed explicitly. Moreover, exact formulas can be found for correlations which means that very precise asymptotics can be computed leading to a deep understanding of what happens to tilings of large regions. Much of the probabilistic behavior observed in these tiling models is expected to appear in much more complicated models that are still exactly solvable, such as the six vertex model, as well as those that are not exactly solvable.

These lectures will concentrate on random domino tilings since they are, by in large, well understood, while still being an active area of research. There are other random tiling models, such as lozenge tilings which share many of the probabilistic features, albeit with a different inherent algebraic structure.

One of the main attractions for researchers to this field has been striking pictures of random tilings of large regions. These simulations have drawn and inspired people from a variety of areas including algebraic combinatorics, probability as well as mathematical physics. Much of the success of the field has been motivated by trying to study these pictures as well as the fact that random tilings are tractable using a wide range of techniques. An example of a random domino tiling can be found in Figure 1, which will be the basis of these notes.

These lectures will only focus on a very limited portion of the theory since it is vast. To this end, we have chosen to restrict to domino tilings of the Aztec diamond, predominantly focussing on uniformly random tilings. Note that we will not address any results on lozenge tilings here, see the excellent book by Gorin [Gor21]. The first lecture will focus on setting up preliniaries, as well as simulating random tilings and Kasteleyn's theorem. The second lecture will introduce determinantal point processes and give methods to find formulas for the correlations of dominoes. The third lecture will briefly highlight some of the general theory, such as the flucutations around the limit shape, and give an example of the saddle point analysis method. We mention that a lot of the preliminaries for these models will follow the setup given in [Joh18].

1.2. **Some Preliminaries.** Let  $\mathcal{G} = (V, E)$  be a finite planar bipartite graph that has no cut points. To each edge, e, associate a weight which is a positive real number, that is  $\nu : E \mapsto \mathbb{R}_+$  is the weight function. A dimer covering of G is

Date: August 2025.



FIGURE 1. A uniformly random domino tiling of an Aztec diamond of size 100

a collection of edges so that each vertex is incident to one edge. The weight of a dimer covering M is defined as

(1) 
$$\nu(M) = \prod_{e \in M} \nu(e)$$

where  $e \in M$  if the edge e is in the dimer covering M.

The dimer model is the probability measure which picks M with probability proportional to w(M). That is, it is the probability measure  $\mathbb{P}$  with

(2) 
$$\mathbb{P}[M] = \frac{\nu(M)}{Z}$$

where  $Z = \sum_{M \in \mathcal{M}} w(M)$  and  $\mathcal{M}$  is the set of all dimer coverings of G. The quantity Z is known as the partition function and  $\mathbb{P}$ , the dimer model measure is an example of a Boltzmann measure.

1.3. **Height function.** Since we have chosen G to be bipartite, we can define a height function on the faces of the graph G. We assume that the graph G is regular, that is the degree of all the vertices are the same. Recall that a bipartite graph means that we can partition the set of vertices into two types. The usual convention for distinguishing between these two types is to assign colors white and black and refer to one type as the white vertices and the other type as the black vertices.

The height function is defined through height differences. The height change on the faces around each white vertex increases by 1 counter clockwise, provided that the incident edge is not covered by a dimer and decreases  $\deg(v) - 1$  if a dimer is crossed, where  $\deg(v)$  denotes the degree of a vertex. For black vertices, it is the same except we interchange counter clockwise with clockwise. An example of a dimer covering with its height function can be found in Figure 2.

We will record some facts that we will not prove. Given a height function on a graph, we can recover the dimer covering by looking for height differences of  $|\deg(v) - 1|$  between adjacent faces. Moreover, dimer coverings and height

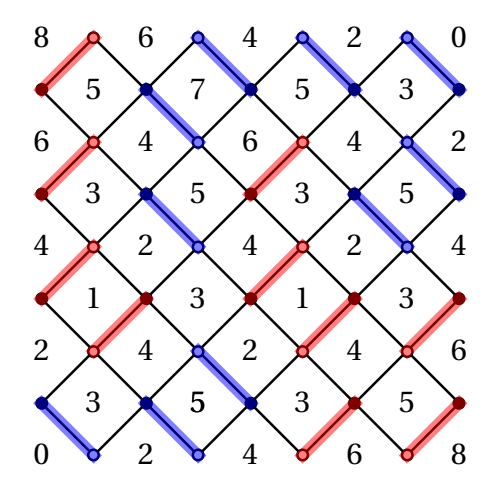


FIGURE 2. An example of a height function, the heights are on the boundary of the region are given.

functions are in one to one correspondence provided an initial height level is set. Finally, a result usually attributed to Thurston [Thu90] is that a region is tileable provided it admits a valid height function. Here, tileable means that a dimer covering can be found and a valid height function is one that has the height difference rules given above.

- 1.4. **Dual Graph.** The dual of a dimer covering gives a tiling. There are two prototypical examples of this: if the underlying graph for the dimer model is (a subgraph of) the honeycomb graph, then the tiling model is a lozenge tiling, whereas if the underlying graph for the dimer model (a subgraph of)  $\mathbb{Z}^2$ , then the tiling model is a domino tiling. These lectures solely focus on domino tilings. We will interchange between dominoes and dimers without mention.
- 1.5. Gauge Transformations and Face weights. The dimer model is parameterized by its *face weights* which are the alternating product of the edge weights around each face. Thus, two dimer models with the same face weights will have the same measure, and are said to be *gauge equivalent*.

If we change the weight function  $\nu$  by multiplying the edge weights incident to a single vertex v by a constant  $\lambda$ , then we change the partition function by a constant  $\lambda$ , but the dimer model measure does not change since exactly one edge is used in each dimer configuration. Such a procedure of multiplying the edge weights around a single vertex is called a gauge transformation.

- 1.6. **Two boundary conditions.** Random tiling models are extremely sensitive to boundary conditions as will be seen later. This was picked up by Kasteleyn in one of the first papers on the dimer model. The two boundary conditions that we will focus on are
  - A  $(2n+1) \times (2m+1)$  region with a corner vertex removed, that is the region  $([0, 2n+1] \times [0, 2m+1] \cap \mathbb{Z}^2) \setminus \{(0, 0)\}.$
  - $\blacklozenge$  An Aztec diamond, introduced in [EKLP92], which we will use the convention that we have rotated by  $\pi/4$ . An Aztec diamond of size n has

white vertices,  $W_n^{Az}$ , given by

 $\{(x_1, x_2) \in \mathbb{Z}^2 : x_1 \mod 2 = 1 \text{ and } x_2 \mod 2 = 0, 1 \le x_1 \le 2n - 1, 0 \le x_2 \le 2n\}$  and black vertices,  $\mathsf{B}_n^{\mathsf{Az}}$ , given by

$$\{(x_1, x_2) \in \mathbb{Z}^2 : x_1 \mod 2 = 0 \text{ and } x_2 \mod 2 = 1, 0 \le x_1 \le 2n, 1 \le x_2 \le 2n-1\}$$

We could generalize the first region to more complicated boundaries, such as those known as Temperleyan regions [KPW00, Rus18, BL23], but we will not do so here. We refer to the boundary conditions as  $\blacksquare$  and  $\blacklozenge$ .

- 1.7. **Sampling.** We give ways to sample dimer coverings of both boundary conditions that are described above. These algorithms are examples of perfect simulations. The first approach can be generalized to the Temperleyan regions, whilst the approach for the Aztec diamond is harder to generalize.
- 1.7.1. Sampling for the boundary condition  $\blacksquare$ . Recall that a tree is a graph that contains no cycles and a spanning tree is a tree which includes all vertices. Temperley's bijection [Tem74] gives a correspondence between dimer coverings on a  $(2m+1) \times (2n+1)$  grid with a corner vertex removed with a pair of directed spanning trees, which we first describe.

Suppose that the white vertices of  $\Lambda = ([0, 2n+1] \times [0, 2m+1] \cap \mathbb{Z}^2) \setminus \{(0, 0)\}$  are given by  $(x_1, x_2)$  such that  $x_1 + x_2 \mod 2 = 0$ . We can split these white vertices into two types, those with  $x_1 \mod 2 = 0$  and those with  $x_2 \mod 2 = 1$ . Label these sets of white vertices  $W_0$  and  $W_1$  respectively.

Prescribe that all the edges incident to vertices in  $W_1$  have weight 1. Then the weight of any matching is given by the dimers incident to vertices in  $W_0$ . For each dimer  $(w, w \pm (0, 1))$  or  $(w, w \pm (1, 0))$  with  $w \in W_i$  and  $i \in \{0, 1\}$ , draw a directed arrow from w to  $w \pm (0, 2)$  or  $w \pm (2, 0)$  respectively. Doing this procedure gives a pair of directed spanning trees. The primal tree, with vertex set given by  $W_0$ , is rooted at (0, 0) while the dual tree, with vertex set given by  $W_1$ , has wired boundary conditions. This procedure is known as Temperley's bijection, since there is a one to one correpondence between trees and dimer configurations.

Wilson's algorithm is a powerful method for generating uniformly random spanning tree. To generate a random spanning tree rooted at the origin, proceed as follows:

- $\bullet$  Consider a random walk with weights given by the edge weights around the  $W_0$  vertices.
- Initially, the tree is empty. Pick a vertex uniformly at random.
- Run the random walk until it hits the root and chronologically erase the loops. This gives a loop-erased random walk. Add this to the tree.
- Pick another vertex uniformly at random not on the tree and perform the above step until all vertices are included in the tree.

The above procedure, known as Wilson's algorithm, generates a random spanning tree, which we will not prove.

The consequence of this means that we can first generate a spanning tree on the  $W_0$  vertices using Wilson's algorithm, which gives the dimers incident to all vertices in  $W_0$  by Temperley's bijection. The remaining dimers are those incident to all vertices in  $W_1$ , which are determined by the dual tree which is already determined.

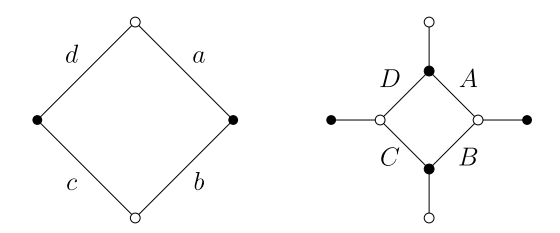


FIGURE 3. The square move and its effect on the edge weights. The left figure shows are square with edge weights a, b, c and d while the right figure shows an application of the square move to that single face. Here, we have  $A = c/\Delta$ ,  $B = d/\Delta$ ,  $C = a/\Delta$ , and  $D = b/\Delta$  where  $\Delta = (ac + bd)$ .

1.7.2. Sampling for the boundary condition  $\blacklozenge$ . To introduce the domino shuffle which gives a powerful method for simulating domino tilings of Aztec diamonds, we require two graphical moves.

- (1) (Square Move)<sup>1</sup> Suppose the edge weights around a square with vertices (0,1), (1,0), (0,-1) and, (-1,0) are given by a,b,c, and d where the labelling is done clockwise around the face starting with the NE edge. We can replace the square by a smaller square with edge weights A, B, C, and D (with the same labelling convention) and add an edge, with edge-weight equal to 1, between each vertex of the smaller square and its original vertex. Then, set  $A = c/\Delta$ ,  $B = d/\Delta$ ,  $C = a/\Delta$ , and  $D = b/\Delta$  where  $\Delta = (ac + bd)$ . This transformation is called the square move; see Fig. 3.
- (2) (Edge contraction) For any two-valent vertex in the graph with incident edges having weight 1, contract the two incident edges. This is called edge contraction.

To describe the domino shuffle [Pro03], we consider an Aztec diamond of size n. We apply the square move on all faces of the Aztec diamond which have coordinates (2i+1,2j+1)  $0 \le i,j \le n-1$ . We contract all the two valent vertices and remove all pendant edges, that is those vertices which are incident to a single vertex (since these vertices must be incident to a dimer). This gives an Aztec diamond of size n-1 but with modified edge weights. We record these edge weights and repeat the procedure on the resulting Aztec diamond and its modified edge weights. Repeat until we reach an Aztec diamond of size 1.

To simulate, we simply run the procedure in reverse and assign two by two dimers on the empty squares with probabilities that were recorded above. That is, for the initial step of a size 1 Aztec diamond, we choose two dimers ((1,0),(0,1)) and ((1,2),(2,1)) with probability given by the weighted Aztec diamond of size 1 found by iteratively applying the square move and edge contraction.

We finish this subsection by leaving a remark that we can consider 0 weights, which would corresponding to freezing off certain dimers. This is achieved by setting the 0 weights to  $\epsilon$  and performing a series expansion when computing the edge weights by the square move; see Figure 5. This extension gives a robust way

<sup>&</sup>lt;sup>1</sup>Usually attributed to Greg Kuperberg

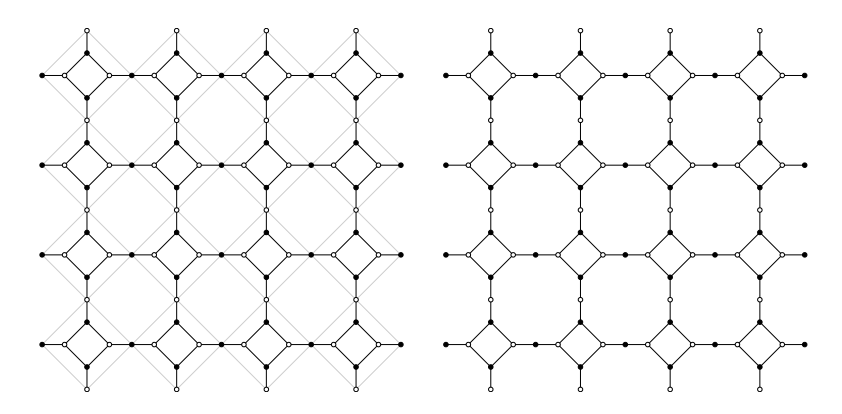


FIGURE 4. An example of the graph transformation after applying the square move on all even faces of an Aztec diamond of size 4. The left figure shows where the square move applied. The figure on the right shows the actual graph. Applying edge contraction to the two-valent vertices and removing pendant edges gives an Aztec diamond of size 3.

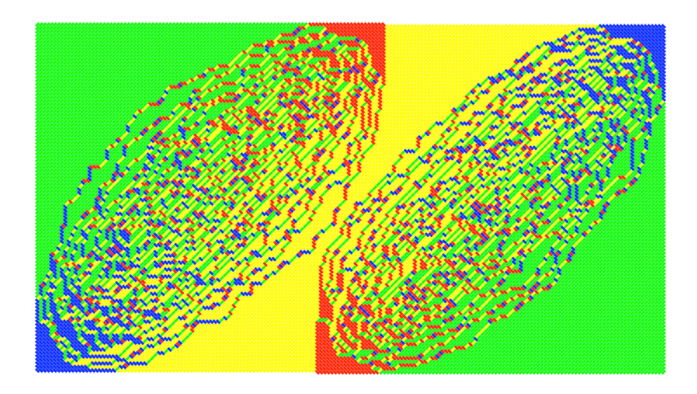


FIGURE 5. A simulation of a double Aztec diamond which gives two limit shapes that touch.

to simulate a larger class of tilings using the domino shuffle, such as embedding lozenge tilings of certain regions within an Aztec diamond.

1.8. **Kasteleyn's Theorem.** Kasteleyn's method gives a method to enumerate the number of tilings as well as compute probabilities of local events.

Let  $\mathcal{G}$  be as above. Let  $\mathbb{W}$  and  $\mathbb{B}$  be the set of white and black vertices respectively. If  $\mathbb{W} = \{w_1, \dots, w_n\}$  and  $\mathbb{B} = \{b_1, \dots, b_n\}$ , then since each edge is incident to both white and black vertices, we can write each dimer configuration as

(3) 
$$C(\sigma) = \{(b_i, w_{\sigma(i)}) : 1 \le i \le n\}$$

for  $\sigma \in S_n$  where  $S_n$  denotes the symmetric group with n symbols. We use the convention that if  $\sigma$  does not correspond to a matching, then  $C(\sigma) = \emptyset$  and

 $\nu((b_i, w_{\sigma(i)})) = 0$  for some i. Then we immediately get that

(4) 
$$Z = \sum_{\sigma \in S_n} \prod_{i=1}^n \nu((b_i, w_{\sigma(i)}))$$

which means that Z is a permanent. To get a determinant, Kasteleyn's observation was to introducing a sign so that the above expansion is equal to a determinant. A Kasteleyn sign is a function  $s: E \to \mathbb{T}$  such that for any face in G with edges  $e_1, \ldots, e_{2k}$  in cyclic order, we have

(5) 
$$\frac{s(e_1)\dots s(e_{2k-1})}{s(e_2)\dots s(e_{2k})} = (-1)^{k+1}$$

and if (bw) is not an edge, then set s((bw)) = 1 by convention. A convenient example for the square grid is to have the vertical edges e have  $s(e) = i = \sqrt{-1}$ . We define the operator  $K : B \to W$  by

(6) 
$$K(b, w) = s((b, w))\nu((b, w)).$$

Given the enumeration of vertices given above, we get the Kasteleyn (-Percus) matrix  $\,$ 

(7) 
$$K = (K(b_i, w_i))_{1 \le i, i \le n}.$$

Then, we get the following theorem, due to Kasteleyn [Kas61, Kas63] as well as Temperley and Fisher [TF61].

**Theorem 1.1.** There is a complex number S with |S| = 1, independent of the choice of edge weights such that  $\det K = SZ$ .

*Proof of Theorem 1.1.* By expanding out the determinant, we get (8)

$$\det K = \sum_{\sigma \in S_n} \operatorname{sgn}(\sigma) \prod_{i=1}^n K(b_i, w_{\sigma(i)}) = \sum_{\sigma \in S_n} \operatorname{sgn}(\sigma) \prod_{i=1}^n s(b_i, w_{\sigma(i)}) \nu((b_i, w_{\sigma(i)})).$$

Write  $S(\sigma) = \operatorname{sgn}(\sigma) \prod_{i=1}^n s((b_i, w_{\sigma(i)})) \nu((b_i, w_{\sigma(i)}))$ . If we can show that  $S(\sigma_1) = S(\sigma_2)$  for all  $\sigma_1, \sigma_2$  such that  $C(\sigma_1), C(\sigma_2) \neq 0$ , then we are done since this would give  $S = S(\sigma)$  and shows that the right side above is a count with a multiplicative factor of S.

Consider two dimer coverings corresponding to  $\sigma_1$  and  $\sigma_2$ . If we overlap these configurations then each vertex is incident to two dimers. This means that the overlapped configuration will consist of loops and double edges where as we traverse around a loop, we alternate between  $\sigma_1$  and  $\sigma_2$  dimers and hence the loops have even length. This means that along each loop, we can rotate the dimers on  $\sigma_1$  so that they overlap with dimers on  $\sigma_2$ , forming double edges.

It is enough to check when  $C(\sigma_1)$  and  $C(\sigma_2)$  differ by a single loop of length 2k and proceed inductively on the remaining loops. In this case, we have that  $\sigma_1 = \sigma_2 \tau$  where  $\tau$  is a permutation equal to the identity except for the k cycle. Let  $e_2, e_4, \ldots, e_{2k}$  be edges covered by dimers in  $C(\sigma_1)$  around the loop and let  $e_1, e_3, \ldots, e_{2k-1}$  be edges covered by dimers in  $C(\sigma_2)$  around the loop. Then we have that

(9) 
$$\frac{S(\sigma_2)}{S(\sigma_1)} = \frac{\operatorname{sgn}(\sigma_2)}{\operatorname{sgn}(\sigma_1)} \prod_{i=1}^n \frac{s(b_i w_{\sigma_2(i)})}{s(b_i w_{\sigma_1(i)})} = \operatorname{sgn}(\tau) \frac{s(e_1) \dots s(e_{2k-1})}{s(e_2) \dots s(e_{2k})} = (-1)^{\ell}$$

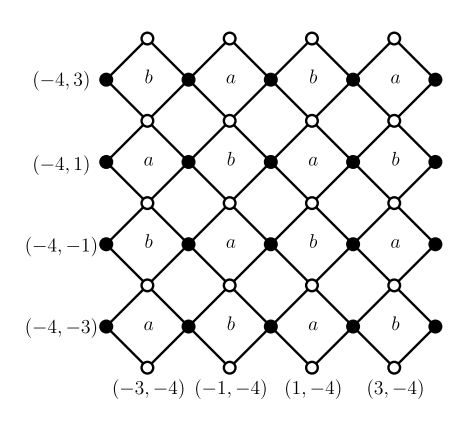


FIGURE 6. An example of a two-periodic Aztec diamond of size 4. Edges incident to faces labelled a have edge weight a while edges incident to faces labelled b have edge weight b. The weights are doubly periodic.

since  $sgn(\tau) = (-1)^k$  and using Exercise 8 below.

One of Kasteleyn's original motivations for enumerating the number of domino tilings was its implications for computing the partition function of the two-dimensional Ising model, since there is a mapping between Ising spin boundaries and the dimer model on certain non bipartite graphs through the *Fisher correspondence*. Since Kasteleyn's theorem can be extended to non bipartite graphs, the partition function for the Ising model can be computed using dimer model techniques; see [Kas63] for more details.

## 1.9. Lecture 1 Exercises.

Exercise 1. Count the number of domino tilings of an 8 by 8 checkerboard with two black squares on opposite corners removed.

**Exercise 2.** Give the height function for a dimer covering of an Aztec diamond of size 4 (your choice of tiling) as well as the height function for the boundary faces.

Exercise 3. Give the height function for a dimer covering of a 5 by 5 portion of the square grid with the bottom left corner removed, including the height function for the boundary faces.

**Exercise 4.** Find the number of dimer coverings of an Aztec diamond of size n by first showing that  $Z_n = 2^{n^2} \tilde{Z}_{n-1}$  where  $Z_n$  is the number of tilings of an Aztec diamond of size n and  $Z_{n-1}$  is the number of tilings of an Aztec diamond of size n-1, but with all the edge weights equal to 1/2.

**Exercise 5.** Compute the partition function of the two-periodic Aztec diamond of size 4m. The weights are given in Figure 6

**Exercise 6.** (Coding exercise) Implement the domino shuffle for the Aztec diamond as well as the sampling for the square grid for all edges having weight 1. Generalize this to arbitrary weights.

**Exercise 7.** (Coding exercise) Sample a dimer covering on a  $(2n+1) \times (2m+1)$  grid with the bottom left corner removed with all edge weights equal to 1.

**Exercise 8.** Consider a planar bipartite graph  $\mathcal{G}$  with no cut points. If a cycle  $e_1, \ldots, e_{2k}$  of length 2k encloses  $\ell$  points in the graph and s(e) is a Kasteleyn sign on  $\mathcal{G}$ , then show that

(10) 
$$\frac{s(e_1)\dots s(e_{2k-1})}{s(e_2)\dots s(e_{2k})} = (-1)^{k+\ell+1}.$$

**Exercise 9.** For an arbitrary choice of faceweights for a square and its neighbouring faces, compute the faceweights after applying the square move.

Exercise 10. Generalize Temperley's bijection in its current setup to the honeycomb graph. What are the allowed boundary conditions?

### 2. Lecture 2

2.1. **Determinantal Point Processes.** Let  $\mathcal{X}$  be a complete separable metric space (e.g.  $\mathbb{R}^d$  or  $\mathbb{Z}^d$ ) and let  $N(\mathcal{X})$  be the space of all boundedly finite counting measures  $\xi$  on  $\mathcal{X}$ . Let  $\lambda$  be a reference measure on  $\mathcal{X}$  (i.e. Lebesgue measure for  $\mathcal{X} = \mathbb{R}^d$ ). We say that  $\xi$  is simple if and only if  $\xi(\{x\}) \leq 1$ .

A point process  $\mathcal{X}$  is a probability measure  $\mathbb{P}$  on  $N(\mathcal{X})$ . We have  $\xi$  is a simple point process if and only if  $\mathbb{P}(\xi \text{ is simple}) = 1$ . For any B bounded we have that the restriction of  $\xi$  to B can be written as  $\sum_{i=1}^{\xi(B)} \delta_{x_i}$  and we think of  $x_i \in \mathcal{X}$  as particles. These particles have no ordering and so the resulting point process can be thought of as a particle process.

Suppose that  $\phi \in L^{\infty}(\mathcal{X}, \lambda)$  and has bounded support B. It is usual to write that

(11) 
$$\prod_{i} (1 + \phi(x_i)) = \prod_{i=1}^{\xi(B)} (1 + \phi(x_i))$$

Then, we define the  $n^{th}$  correlation function  $\rho_n$  through

(12) 
$$\mathbb{E}[\prod_{i} (1 - \phi(x_i))] = \sum_{n=0}^{\infty} \frac{(-1)^n}{n!} \int_{\mathcal{X}^n} \prod_{j=1}^n \phi(x_j) \rho_n(x_1, \dots, x_n) d^n \lambda(x),$$

where the n=0 term on the sum on right side above is equal to 1 provided that

(13) 
$$\sum_{n=0}^{\infty} \frac{\|\phi\|_{\infty}^n}{n!} \int_{\mathcal{X}^n} \rho_n(x_1, \dots, x_n) d^n \lambda(x) < \infty.$$

The interpretation of the correlation function is as follows

- If  $\mathcal{X}$  is discrete, then  $\rho_n(x_1,\ldots,x_n)$  is the probability of seeing particles at  $x_1,\ldots,x_n$ .
- If  $\mathcal{X}$  is continuous, then  $\rho_n(x_1,\ldots,x_n)$  is the density of particles at  $x_1,\ldots,x_n$ .

A determinantal point process is defined as

(14) 
$$\rho_n(x_1, \dots, x_n) = \det K(x_i, x_i)_{1 \le i, i \le n}$$

and K is a correlation kernel. With the above equation, (12) becomes

(15) 
$$\mathbb{E}[\prod_{i} (1 - \phi(x_i))] = \sum_{n=0}^{\infty} \frac{(-1)^n}{n!} \int_{\mathcal{X}^n} \prod_{i=1}^n \phi(x_i) \det(K(x_i, x_j))_{1 \le i, j \le n} d^n \lambda(x).$$

The correlation kernel K can be viewed as an integral kernel of an operator K on  $L^2(\mathcal{X}, \lambda)$ , that is

(16) 
$$(Kf)(x) = \int_{\mathcal{X}} K(x, y) f(y) d\lambda(y)$$

provided that the operator is well-defined. Suppose that  $\phi \in L^{\infty}(\mathcal{X}, \lambda)$  has bounded support B. Then, (15) becomes

(17) 
$$\mathbb{E}\left[\prod_{i}(1-\phi(x_{i}))\right] = \sum_{n=0}^{\infty} \frac{(-1)^{n}}{n!} \int_{B^{n}} \prod_{j=1}^{n} \phi(x_{j}) \det(K(x_{i}, x_{j}))_{1 \leq i, j \leq n} d^{n} \lambda(x)$$

provided that

(18) 
$$\sum_{n=0}^{\infty} \frac{\|\phi\|_{\infty}^n}{n!} \left| \int_{B^n} \det(K(x_i, x_j))_{1 \le i, j \le n} d^n \lambda(x) \right| < \infty.$$

The expansion in (17) is the definition of the Fredholm determinant  $\det(\mathbb{I} + \mathbb{I}_B K \mathbb{I}_B \phi)_{L^2(\mathcal{X})} = \det(\mathbb{I} + K\phi)_{L^2(B)}$ , where  $K\phi$  is an integral operator on  $L^2(B)$  with kernel  $K(x,y)\phi(y)$ . Although there are other definitions which are equivalent provided that the operator is trace class, this is the most covenient one for these lectures. Appropriate choices of  $\phi$  will give useful statistics for determinantal point process, with examples including gap probabilities, height functions, etc.

Determinantal point processes were first identified by Macchi [Mac75] and have a long history in random matrix theory. They have played an important and significant role in models in *integrable probability*, such as random tiling models, last passage percolation, TASEP and uniform spanning tree; for example see [Joh06, Bor10, Sos00] for further details as well as details on constructions and properties. The term determinantal was coined by Borodin in [BO00] and has since become standard.

2.2. **Inverse Kasteleyn Matrix.** The following theorem is due to Kenyon [Ken97] as well as Montroll-Potts-Ward [MPW63].

**Theorem 2.1.** Let  $e_1 = (b_1, w_1), \ldots, e_r = (b_r, w_r)$ . Then, the probability  $e_1, \ldots, e_r$  are observed in a dimer covering is given by

(19) 
$$\mathbb{P}[e_1, \dots, e_r] = \prod_{i=1}^r K(b_i, w_i) \det(K^{-1}(w_i, b_j))_{1 \le i, j \le r}.$$

That is, the dimers form a determinantal point process on the edges with correlation kernel given by  $L(e_i, e_j) = K(b_i, w_i)K^{-1}(w_i, b_j)$ .

*Proof.* For a dimer cover M, let

(20) 
$$\mathbb{I}_M(e) = \begin{cases} 1 & \text{if } e \in M \\ 0 & \text{if } e \notin M. \end{cases}$$

Then, we have that  $Z = \sum_{M \in \mathcal{M}} \prod_{e \in M} \nu(e)^{\mathbb{I}_M(e)}$ . We proceed by differentiating the partition functon in this form. Indeed, we have that

(21)
$$\mathbb{P}[e_{1}, \dots, e_{r}] = \frac{1}{Z} \sum_{M \in \mathcal{M}} \prod_{i=1}^{r} \mathbb{I}_{M}(e_{i}) \prod_{e \in M} \nu(e)$$

$$= \frac{1}{Z} \sum_{M \in \mathcal{M}} \prod_{i=1}^{r} \mathbb{I}_{M}(e_{i}) \nu(e_{i}) \prod_{\substack{e \in M \\ e \neq e_{i} \forall 1 \leq i \leq r}} \nu(e)$$

$$= \frac{1}{Z} \prod_{i=1}^{r} \nu(e_{i}) \frac{\partial^{r} Z}{\partial \nu(e_{1}) \dots \partial \nu(e_{r})}$$

$$= \frac{1}{\det K} \prod_{i=1}^{r} \nu(e_{i}) \frac{\partial^{r} \det K}{\partial \nu(e_{1}) \dots \partial \nu(e_{r})}$$

where in the last line we have used Theorem 1.1 and the fact that the signs

Let  $I = \{i_k\}_{k=1}^r$ ,  $J = \{j_k\}_{k=1}^r$  and  $e_i = (b_{i_k}, w_{i_k})$ . Let  $I^{\complement} = \{1, \dots, n\} \setminus I$  and  $J^{\complement}$  be defined similar. Note that  $K(b_{i_k}, w_{j_k}) = s((b_{i_k}, w_{j_k})) \nu((b_{i_k}, w_{j_k}))$ . Using Laplace's expansion we get that

(22) 
$$\frac{\partial^r \det K}{\partial v(e_1) \dots \partial v(e_r)} = (-1)^{\sum_{i \in I} i + \sum_{j \in J} j} \det K(I^{\complement}, J^{\complement}) \prod_{i=1}^r s(e_i)$$

Substituting back into (21) and noting that by the formula for inverting matrices we have

$$(23) \qquad (-1)^{\sum_{i \in I} i + \sum_{j \in J}} \frac{\det K(I^{\complement}, J^{\complement})}{\det K} = \det K^{-1}(J, I).$$

The result follows.

In what follows below, we give a couple of methods for computing the inverse of the Kasteleyn matrix for the Aztec diamonds, the second of which is systematic.

2.3. Computing the inverse Kasteleyn matrix for the Aztec diamond. Here we give a combinatorial method for computing the inverse Kasteleyn matrix for an Aztec diamond of size n. Let  $e_1 = (1,1)$  and  $e_2 = (-1,1)$ . We will consider the Kasteleyn matrix

(24) 
$$K_n^{\text{Az}}(x,y) = \begin{cases} 1 & \text{if } x = y \pm e_1 \\ i & \text{if } x = y \pm e_2 \\ 0 & \text{otherwise} \end{cases}$$

where  $x \in \mathsf{B}_n^{\mathsf{Az}}$ ,  $y \in \mathsf{W}_n^{\mathsf{Az}}$  and  $\mathsf{i} = \sqrt{-1}$ . We can apply  $(K_n^{\mathsf{Az}})$  to  $(K_n^{\mathsf{Az}})^{-1}$  entrywise which leads to a linear equation expressing  $(K_n^{\mathsf{Az}})^{-1}(x,y)$  in terms of its neighbouring vertices since  $(K_n^{\mathsf{Az}})$  is a sparse matrix. More preciesely, we have that for  $x, y \in B_{Az}$ , we have

$$((K_n^{\text{Az}}).(K_n^{\text{Az}})^{-1})(x,y) = (K_n^{\text{Az}})^{-1}(x+e_1,y)\delta_{x_1<2n} + (K_n^{\text{Az}})^{-1}(x-e_1,y)\delta_{x_1>0} + \mathrm{i}(K_n^{\text{Az}})^{-1}(x+e_2,y)\delta_{x_2<2n} = \delta_{x=y}.$$

A similar equation can be found by postmultplying  $(K_n^{\text{Az}})^{-1}$  by  $(K_n^{\text{Az}})$ . Both of these equations can be solved using generating functions which gives a generating function formula for  $(K_n^{\text{Az}})^{-1}$  which is dependent on the boundary of the Aztec diamond, that is a function of  $(K_n^{\text{Az}})^{-1}(x,y)$  where x is either of the form (2i+1,0) or (2i+1,2n) and y is either of the form (0,2j+1) or (2n,2j+1) for  $0 \le i,j \le n-1$ . This approach works for more general weightings as well as general graphs, which means that once  $(K_n^{\text{Az}})^{-1}$  is established for its boundary values, the interior values will follow from a linear recurrences.

2.3.1. Boundary recurrence. If w and b are on the same face (including the boundary face), then  $|K^{-1}(w,b)| = Z(\{w,b\})/Z$  where  $Z(\{w,b\})$  is the partition function obtained from moving w and b from the graph, which follows from Cramers Rule. The overall sign of  $K^{-1}(w,b)$  can easily be computed. Below we give a recusion for computing a ratio of partition functions of the Aztec diamond with the top partition function having a pair of vertices removed from the boundary.

Let  $Z_n(i,j)$  denote  $|K_{Az}^{-1}((2i+1,0),(0,2j+1))\det(K_n^{Az})|$  and  $Z_n = \det(K_n^{Az})$  where  $(K_n^{Az})$  is the Kastelyn matrix for the Aztec diamond defined in (24). Then we have the following lemma

**Lemma 2.2.** For  $0 \le i, j \le n - 1$ , we have

$$(26) \qquad \frac{Z_n(i,j)}{Z_n} = \frac{1}{2} \sum_{\substack{k,l \in \{0,1\}\\ (i-k,j-l) \neq (-1,-1)}} \frac{Z_{n-1}(i-k,j-l)}{Z_{n-1}} + \frac{1}{2} \delta_{(i,j)=(0,0),n \ge 1}$$

Proof. Notice that  $Z_n(i,j)$  is equivalent to adding a pendent edge to (2i+1,0) and another pendent edges (0,2j+1). With this in mind, we apply the square move given in the first lecture which gives an Aztec diamond of size n-1, with all diagonal edges having weight equal to  $\frac{1}{2}$  and all the remaining vertical and horizontal edges having weight 1. Some care needs to be applied when removing the pendant edges - we can remove the pendent vertices along with their incident edges for the vertices

- (2k+1,0) for  $0 \le k \le n-1$  but  $k \ne i$ ,
- (0, 2l+1) for  $0 \le l \le n-1$  but  $l \ne j$ ,
- (2k+1,2n) for  $0 \le k \le n-1$  and (2n,2l+1) for  $0 \le l \le n-1$ .

We apply edge contraction at the two valent vertices that are incident to two horizontal or two vertical edges; see Figure 7. We get that (27)

$$Z_n(i,j) = \sum_{k \in \{i-1,i\} l \in \{j-1,j\}} \frac{1}{4} \tilde{Z}_{n-1}(k,l) 2^{n^2} \delta_{0 \le k \le n-2} \delta_{0 \le l \le n-2} + \frac{1}{2} \delta_{(i,j)=(0,0)} \tilde{Z}_{n-1} 2^{n^2}$$

where  $\tilde{Z}_{n-1}(k,l)$  is denotes the partition function of the Aztec diamond of size n-1 with all edges having weight 1/2 and removing (2k+1,0) and (0,2l+1) from the graph. The above equation follows by carefully considering the possible matchings from the previous added pendent edges and noting that when (i,j) = 0 and (k,l) = (-1,-1), then the resulting configuration is simply an Aztec diamond of size n-1 with edge weight 1/2 and the additional factor of 1/2 comes from the forcing of the bottom leftmost diagonal edge.

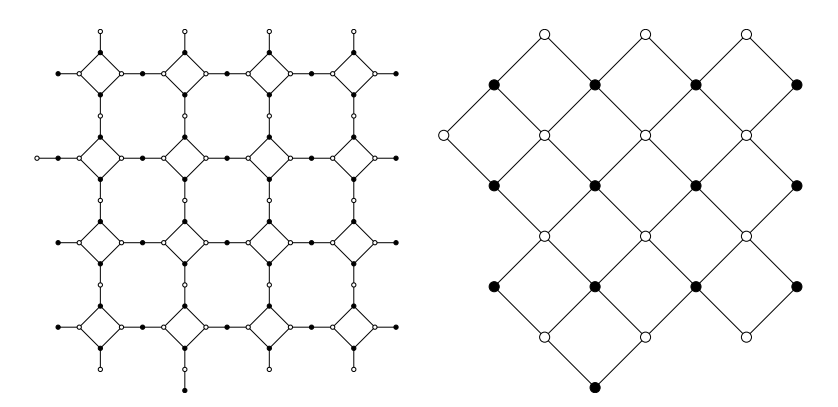


FIGURE 7. The effect of applying the shuffle on Aztec diamond of size 4 with an additional pendant edge. The bottom black vertex has two choices of dimers and so does the leftmost white vertex which leads to a sum.

We divide the above equation by  $Z_n$  use Exercise 4 to get

$$(28) \ \frac{Z_n(i,j)}{Z_n} = \sum_{k \in \{i-1,i\} l \in \{j-1,j\}} \frac{1}{4} \frac{\tilde{Z}_{n-1}(k,l)}{\tilde{Z}_{n-1}} 2^{n^2} \delta_{0 \le k \le n-2} \delta_{0 \le l \le n-2} + \frac{1}{2} \delta_{(i,j)=(0,0)}$$

The last step is to apply a gauge transformation that multiplies all the white vertices by 2 for the both the numerator and denominator of the first term in the right side of the above equation. The result then follows after resumming.  $\Box$ 

The above method for computing the inverse Kasteleyn matrix was introduced in [CY14] with a goal of studying the two-periodic Aztec diamond, whose inverse was also computed in that paper. Since this paper, there have been more systematic ways to compute the correlation kernels for doubly periodic weights of which the two-periodic Aztec diamond is one of. Only one of these methods, using the matrix valued orthogonal polynomials has been generalized to doubly periodically weighted lozenge tilings [Kui24].

2.4. **Non-intersecting lattice paths.** Associated to each tiling of an Aztec diamond, there is a non-intersecting path description, sometimes known as the DR paths.

The vertex set for the non-intersecting lattice paths is given by  $\{(2j,2k): 0 \le j \le n, 0 \le k \le n\} \setminus \{(0,0)\}$  and at each vertex v, there are directed edges (v,v+(2,0)), (v,v+(2,-2)) and (v,v+(0,-2)). The correspondence between dimers and paths is given by

- if a dimer covers the edge ((2i, 2j+1), (2i+1, 2j)), then there is a directed edge ((2i, 2j+2), (2i+2, 2j)),
- if a dimer covers the edge ((2i, 2j + 1), (2i + 1, 2j + 2)), then there is a directed edge ((2i, 2j + 2), (2i + 2, 2j + 2)),
- if a dimer covers the edge ((2i+1,2j),(2i+2,2j+1)), then there is a directed edge ((2i+2,2j+2),(2i+2,2j))

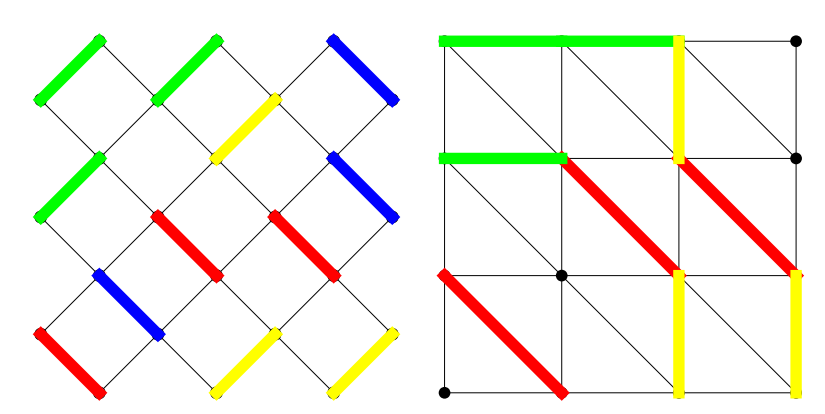


FIGURE 8. The correspondence between an Aztec diamond and DR-paths.

for  $0 \le i, j \le n-1$ . Note that there is no path if there is a dimer of the form ((2i+2,2j+1),(2i+1,2j+2)) for  $0 \le i,j \le n-1$ . Figure 8 shows an example.

2.5. **LGV Theorem.** Let  $\mathcal{G} = (V, E)$  be a directed, acyclic graph with no mulitple edges. Let  $\Pi(u, v)$  be all directed paths  $\pi$  from u to v. Let  $\Pi(\underline{u}, \underline{v})$  be all directed paths  $(\pi_1, \ldots, \pi_n)$  from  $\underline{u} = (u_1, \ldots, u_n)$  to  $\underline{v} = (v_1, \ldots, v_n)$ . We say that two paths intersect if they share a common vertex, otherwise they are non-intersecting. Let  $w: E \to \mathbb{C}$  be the weight function and set

$$w(\pi) = \prod_{e \in \pi} w(e)$$

and

$$w(\pi_1, \dots, \pi_n) = \prod_{i=1}^n w(\pi_i).$$

Let  $\mathcal{F}$  be a family of paths and write

(29) 
$$W(\mathcal{F}) = \sum_{(\pi_1, \dots, \pi_n) \in \mathcal{F}} w(\pi_1, \dots, \pi_n)$$

Let

$$p(u,v) = W(\Pi(u,v)) = \sum_{\pi \in \Pi(u,v)} w(\pi)$$

which is the trnasition weight from u to v. We say that a path is  $\mathcal{G}$ -compatible if  $\alpha < \alpha'$  and  $\beta > \beta'$ , if every path  $u_{\alpha} \to v_{\beta}$  intersect every path  $u_{\alpha'}$  to  $v_{\beta'}$ . The LGV theorem states that for every  $\mathcal{G}$ -compatible paths,  $W(\Pi_{n.i.}(u,v) = \det p(u_i,v_j)_{1\leq i,j\leq n}$ , where  $\Pi_{n.i.}$  are the paths that are non-intersecting. The matrix inside the determinant is often called the LGV Matrix.

2.6. Relationship between Kasteleyn matrix and LGV Theorem. We assign a specific ordering to the white and black vertices, which are given by the functions  $w_n^{Az} : [n(n+1)] \to \mathbb{W}_n^{Az}$  and  $b_n^{Az} : [n(n+1)] \to \mathbb{B}_n^{Az}$  where

functions 
$$w_n^{\text{Az}}: [n(n+1)] \to \mathbb{W}_n^{\text{Az}}$$
 and  $b_n^{\text{Az}}: [n(n+1)] \to \mathbb{B}_n^{\text{Az}}$  where
$$(30) \qquad w_n^{\text{Az}}(i) = \begin{cases} (2i-1,0) & \text{if } 1 \leq i \leq n \\ (2[i-1]_n+1,2n+2-2\lfloor \frac{i-1}{n} \rfloor) & \text{otherwise} \end{cases}$$

and

$$(31) \qquad b_n^{\operatorname{Az}}(i) = \left\{ \begin{array}{ll} (0,2i-1) & \text{if } 1 \leq i \leq n \\ (2[i-1]_n+2,2n+1-2\lfloor \frac{i-1}{n} \rfloor) & \text{otherwise} \end{array} \right.$$

for  $1 \le i \le n(n+1)$ , where  $[i]_n = i \mod n$ .

Let  $W_n^{\text{Az}} = (w_{ij})_{1 \leq i,j \leq n}$  with  $w_{ij}$  equal to the number of DR paths from (0,2i) to (2j,0) for  $1 \leq i,j \leq n$  which is enumerated by the LGV theorem. Due to the one-to-one correspondence with dimer coverings,  $\det W_n^{\text{Az}}$  is also equal to the number of dimer coverings on the Aztec diamond.

For a matrix M, denote M[i; j, k; l] to be the submatrix of M restricted to rows i through to j and columns k through to l.

**Lemma 2.3.** Let  $A_n = (K_n^{Az})[1; n, 1; n]$ ,  $B_n = (K_n^{Az})[1; n, n+1; n(n+1)]$ ,  $C_n = (K_n^{Az})[n+1; n(n+1), 1; n]$  and  $D_n = (K_n^{Az})[n+1; n(n+1), n+1; n(n+1)]$ . For  $1 \le i, j \le n$ , let

$$\tilde{w}_{ij} = (A_n - B_n D_n^{-1} C_n)(i, j)$$

and  $\tilde{W}_n^{Az} = (\tilde{w}_{ij})_{1 \leq i,j \leq n}$ . Then we have  $w_{ij} = |\tilde{w}_{ij}|$ .

*Proof.* We have that

(32) 
$$\det K_n^{Az} = \det(A - BD^{-1}C) \det D$$

provided that D is invertible. It is immediate that D has only one tiling. The remainder of the proof involves showing the following claim whose proof is an exercise.

Claim 1. The matrix  $(A - BD^{-1}C)_{ij}$  is exactly equal (up to sign), the  $(i, j)^{th}$  entry of the LGV matrix.

# 2.7. Computing the Correlation Kernel.

2.7.1. Setup using the LGV Theorem. The first step is to extend the graph for the non-intersecting lattice paths. The new vertex set is given by  $\{(j,k): 0 \le j \le 2n, 0 \le k \le n\} \setminus \{(0,0)\}$ . At each vertex v of the form (2j,k), there are directed edges (v,v+(1,0)), (v,v+(1,-1)) and (v,v+(0,-r)) for  $0 \le j,k \le n$  and  $r \ge 0$  while at each vertex v of the form (2j+1,k), there is a directed edge (v,v+(1,0)) for  $0 \le j,k \le n$ . The relationship with dimers is given as follows:

- if a dimer covers the edge ((2i,2j+1),(2i+1,2j)), then there is a directed edge ((2i,j+1),(2i+1,j)) and another directed edge ((2i+1,j),(2i+2,j)),
- if a dimer covers the edge ((2i, 2j + 1), (2i + 1, 2j + 2)), then there is a directed edge ((2i, j + 1), (2i + 1, j + 1)) and another directed edge ((2i + 1, j + 1), (2i + 2, j + 1)),
- if a dimer covers the edge ((2i+1,2j),(2i+2,2j+1)), then there is a directed edge ((2i+2,j+1),(2i+2,j))

for  $0 \le i, j \le n-1$ . As before, there is no path if there is a dimer of the form ((2i+2,2j+1),(2i+1,2j+2)) for  $0 \le i, j \le n-1$ . By construction, the particle starting at (0,n-i) will end at (2n,-i) for  $1 \le i \le n$ .

To make the analysis simpler, we assert that the edges ((2i, j), (2i + 1, j - 1)) and ((2i, j + 1), (2i, j)) have weight  $a^{-1}$  and a respectively, where  $a \in (0, 1)$ . This

is gauge equivalent to having the dimers that are parallel to (1,1) having weight a. The transition functions are then given by

$$p_{2i,2i+1}(x,y) = a^{-1}\delta_{x-1=y} + \delta_{y=x}$$

and

$$p_{2i+1,2i+2}(x,y) = a^{x-y} \delta_{x-y \ge 0}$$

for  $0 \le i \le n$ . We extend the process for M paths with the paths from n+1 to M, counting from the top, having a deterministic configuration. The random configuration of paths induces a natural point process  $\{(i, x_j^i\}_{i=0,j=1}^{2n,M} \text{ where } (i, x_j^i) \text{ is the lowest vertex in the } j^{th} \text{ path at the vertical section with horizontal coordinate } i$ 

Then, by the LGV theorem applied multiple times, the probability of seeing a configuration x is proportional to

(33) 
$$p_{0,2n}(x) = \prod_{r=0}^{2n-1} \det p_{r,r+1}(x_j^r, x_k^{r+1})_{1 \le j,k \le M}.$$

It is convenient to work with Fourier coefficients. Consider  $p_{r,r+1}(x,y) = \hat{\phi}_r(y-x)$ , that is

(34) 
$$p_{r,r+1}(x,y) = \frac{1}{2\pi i} \int_{\gamma_1} \frac{dz}{z} \frac{\phi_r(z)}{z^{y-x}}$$

where  $\gamma_r$  is a positively oriented contour around the origin of radius r. In our case, we have

(35) 
$$\phi_{2i,2i+1}(z) = 1 + a^{-1}z^{-1}$$
 and  $\phi_{2i+1,2i+2}(z) = \frac{1}{1 - az^{-1}}$ 

Define

(36) 
$$\phi_{2r+\varepsilon_1,2s+\varepsilon_2}(z) = (1+a^{-1}z^{-1})^{s-r+\varepsilon_2-\varepsilon_1} \frac{1}{(1-az^{-1})^{s-r}}$$

so that

(37) 
$$p_{r,s}(x,y) = \hat{\phi}_{r,s}(y-x)\mathbb{I}_{r < s}.$$

Let  $W_{i,j} = p_{0,2n}(n-i,-j)$  for  $1 \le i,j \le M$ . The Eynard Mehta Theorem states that the correlation kernel of particles is given by

$$L((2r + \varepsilon_1, u); (2s + \varepsilon_2, v)) = -p_{2r + \varepsilon_1, 2s + \varepsilon_2}(u, v)$$

(38) 
$$+ \sum_{i,j=1}^{n} p_{2r+\varepsilon_1,2n}(u,-j)(W^{-1})_{ji}p_{0,2s+\varepsilon_2}(n-i,v).$$

We have the following lemma.

**Lemma 2.4.** For  $a < \rho_1 < \rho_2 < 1/a$ ,

$$L((2r+\varepsilon_1, u); (2s+\varepsilon_2, v)) = -\frac{\mathbb{I}_{2r+\varepsilon_1 < 2s+\varepsilon_2}}{2\pi i} \int_{\gamma_{\rho_1}} \frac{dz}{z} \frac{(1+a^{-1}z^{-1})^{s-r+\varepsilon_2-\varepsilon_1}}{(1-az^{-1})^{s-r}} \frac{1}{z^{v-u}} + \frac{1}{(2\pi i)^2} \int_{\gamma_{\rho_1}} dz \int_{\gamma_{\rho_2}} dw \frac{z^u}{w^{v+1}(w-z)} \frac{(1+a^{-1}z^{-1})^{n-r-\varepsilon_1}(1-az^{-1})^r}{(1-aw^{-1})^s(1+a^{-1}w)^{n-s-\varepsilon_2}}.$$

We leave the proof of this lemma as an exercise.

In general, computing the inverse of W is difficult, but there are tricks such as noticing that W is a finite Toeplitz matrix. There are inversion formulas for infinite Toeplitz matrices, so the standard approach is to show that W can be made into an infinite Toeplitz matrix by freezing off configurations. Once the inverse of W is found, then the correlation kernel is essentially determined. In fact, this also determines the inverse Kasteleyn matrix through the Schur complement formula; see Lemma 2.3.

The approach mentioned briefly above has been used to compute the correlation kernel of many so called integrable probability models, including uniformly random domino tilings [Joh05]. For higher periodic weights on the Aztec diamond, three main methods [CY14, DK21, BD19] have been established with relations between the methods found in [CD23, KP25]. Nevertheless, the problem of finding the correlation kernel for more general weights was recently settled [BdT24] in full generality by exploiting an inherent algebraic structure of the general weights.

#### 2.8. Lecture 2 Exercises.

**Exercise 11.** Let a and c be white vertices on the boundary of the Aztec diamond and let b and d be black vertices on the boundary of the Aztec diamond. Impose that a, b, and c and d have cyclic order around the boundary. Let  $Z_n[\{v_1,\ldots,v_m\}]$  denote the partition function of removing  $v_1,\ldots,v_m$  from the Aztec diamond. Show that

(40) 
$$Z_n[\{a,b,c,d\}]Z_n = Z_n[\{a,b\}]Z_n[\{c,d\}] + Z_n[\{a,d\}]Z_n[\{b,c\}]$$

This is known as *Kuo condensation* [Kuo06].

Exercise 12. Show Claim 1.

Exercise 13. Prove that the DR paths defined in Section 2.4 are non-intersecting paths.

Exercise 14. Prove Lemma 2.4.

**Exercise 15.** Find the boundary recurrence relation for the two-periodic Aztec diamond.

# 3. Lecture 3

3.1. **Kenyon-Okounkov-Sheffield Theory.** We give a brief excursion into some general model theory discovered in [KOS06] which determines the translation invariant Gibbs measures for dimer models on the plane with a specified slope. We will only describe the results as the proofs are not the focus of these notes; see [KOS06] for details.

We will consider the theory for the two-periodic weighting of the square grid. Here, there are two types of white vertices and two types of black vertices. Let

(41) 
$$\tilde{W} = \{(i, j) \in \mathbb{Z}^2 : i \mod 2 = 1, j \mod 2 = 0\},\$$

denote the white vertices,

(42) 
$$\tilde{B} = \{(i, j) \in \mathbb{Z}^2 : i \mod 2 = 0, j \mod 2 = 1\},$$

denote the black vertices, and for  $i \in \{0, 1\}$ , let

(43) 
$$\tilde{\mathbf{B}}_i = \{ (x_1, x_2) \in \tilde{\mathbf{B}} : x_1 + x_2 \mod 4 = 2i + 1 \}$$

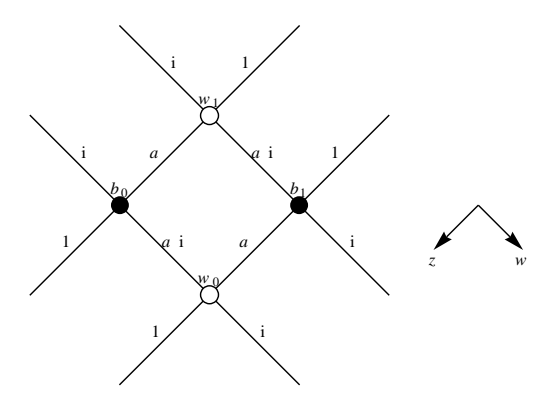


FIGURE 9. The fundamental domain of the two-periodic weighting.

and

(44) 
$$\tilde{\mathbf{W}}_i = \{ (x_1, x_2) \in \tilde{\mathbf{W}} : x_1 + x_2 \mod 4 = 2i + 1 \}$$

denote the two types of white and black vertices respectively.

The results of [KOS06] rely on using the smallest non-repeating unit of the graph which is called the *fundamental domain*, which in our case is depicted in Figure 9 along with the edge weights and Kasteleyn signs.

To describe the Gibbs measure, introduce magnetic coordinates. For the fundamental domain considered here, we represent the magnetic coordinates by  $(B_1, B_2)$  where each edge weight in the neighboring fundamental domain in the direction (1,1) (or resp. (1,-1)), is mulitplied by  $e^{B_1}$  (or  $e^{B_2}$  resp.). Conversely, each edge weight in the neighboring fundamental domain in the direction -(1,1) (or -(1,-1) resp.) is multiplied by  $e^{-B_1}$  (or  $e^{-B_2}$  resp.). These magnetic coordinates are related to the average slope, that is, the Gibbs measures are characterized by the magnetic coordinates. For example,  $B_1 = 0$  and  $B_2 = 0$  correspond to zero average slope in both directions.

Let K(z, w) denote the Kasteleyn matrix for the above fundamental domain where 1/z is the multiplicative factor when crossing to a fundamental domain in the direction  $e_1$  and 1/w is multiplicative factor when crossing to the fundamental domain in the direction  $e_2$ ; see Figure 9. Explicitly, we have

(45) 
$$K(z,w) = \begin{pmatrix} i(a+w^{-1}) & a+z \\ a+z^{-1} & i(a+w) \end{pmatrix}.$$

Suppose that  $x \in \widetilde{\mathbb{W}}_{\alpha_1}$  and  $y \in \widetilde{\mathbb{B}}_{\alpha_2}$  for  $\alpha_1, \alpha_2 \in \{0, 1\}$  with the translation to get to the fundamental domain containing y from the fundamental domain containing x given by  $ue_1 + ve_2$ . The whole plane inverse Kasteleyn matrix for the entries x and y with magnetic coordinate ( $\log r_1, \log r_2$ ) is denoted by  $\mathbb{K}_{r_1, r_2}^{-1}(x, y)$ . Then from [KOS06], we have

(46) 
$$\mathbb{K}_{r_1,r_2}^{-1}(x,y) = \frac{1}{(2\pi i)^2} \int_{\Gamma_{r_1}} \frac{dz}{z} \int_{\Gamma_{r_2}} \frac{dw}{w} [(K(z,w))^{-1}]_{\alpha_1+1,\alpha_2+1} z^u w^v,$$

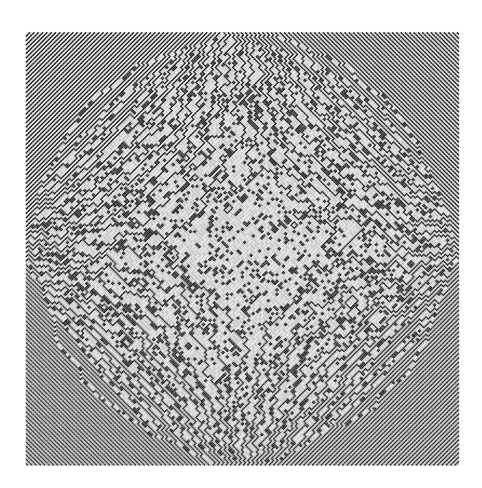


FIGURE 10. A simulation of a two-periodic Aztec diamond of size 200, showing three macroscipic regions

where  $\Gamma_r$  denotes a positively oriented contour around 0 with radius r. In the above formula,  $(K(z, w))^{-1}$  is the inverse of K(z, w) and is given explicitly by

(47) 
$$(K(z,w))^{-1} = \frac{1}{P(z,w)} \begin{pmatrix} i(a+w) & -(a+z) \\ -(a+z^{-1}) & i(a+w^{-1}) \end{pmatrix}$$

where

(48) 
$$P(z,w) = \det K(z,w) = -2 - 2a^2 - \frac{a}{w} - aw - \frac{a}{z} - az.$$

The function P(z, w) is called the *characteristic polynomial* and the theory goes further too. Look at the exponents of P(z, w) and plot the Newton polygon. Then, the interior integer points corresponds to smooth regions, the exterior integer points are frozen regions while the remaining interior points (that are not integer points) correspond to the rough regions, which are all parameterized by the average slope. Here, frozen corresponds to deterministic configurations, rough corresponds to polynomial decay of correlations with distance between dominoes and smooth correspond to exponential decay of correlations with distance between dominoes.

In the two-periodic weighting case, there is one smooth region with magnetic coordinates are given by (0,0) (the average slope is zero), while if the magnetic coordinates are given by  $(\log r_1, \log r_2)$  with P(z,w) = 0 for some  $(z,w) \in \Gamma_{r_1} \times \Gamma_{r_2}$  (from [KOS06] the value of  $(z,w) \in \Gamma_{r_1} \times \Gamma_{r_2}$  with P(z,w) = 0 is complex), then the model is in a rough region. An example of simulation of the two-periodic weighting for the Aztec diamond, that is the two-periodic Aztec diamond, is given in Figure 10 which shows three macroscopic regions.

Finally, we make a remark taht in this mini-course, we have omitted several topics that are central to the general dimer model machinery One of the most fundamental results omitted is the variational principle for the dimer model [CKP01], which states that a continuous surface emerges for large random dimer coverings representing the bulk shape of the region. This surface is called the limit shape and it is the minimizer of the so-called surface tension. Associated to

the limit shape are the limit shape curves which splits the tiling into potentially three macroscopic regions as determined in [KOS06]. Studying the limit shape through its minimizer is a hard problem but has given a deep understanding of the theory of dimer models [KO07, ADPZ20] such as the limit shape curves are algebraic. Aside from uniformly random lozenge tilings [Agg23], the local limits in random tilings models to their corresponding Gibbs measure counterparts has only been established where there are explicit formulas for the correlation kernel.

3.2. **The Airy Process.** The Airy process is a collection of stochastic processes expected to govern the long time, large scale, spatial fluctuations of random growth models. We define it through its point process.

Define the extended Airy kernel as

(49) 
$$\mathcal{A}(\tau,\xi;\sigma,\eta) = \begin{cases} \int_0^\infty e^{-\lambda(\tau-\sigma)} \operatorname{Ai}(\xi+\lambda) \operatorname{Ai}(\eta+\lambda) d\lambda & \text{if } \tau \ge \sigma \\ -\int_0^\infty e^{-\lambda(\tau-\sigma)} \operatorname{Ai}(\xi+\lambda) \operatorname{Ai}(\eta+\lambda) d\lambda & \text{if } \tau \ge \sigma \end{cases}$$

where  $Ai(\cdot)$  is the Airy function which is defined by

(50) 
$$\operatorname{Ai}(x) = \frac{1}{2\pi i} \int_{\mathcal{C}} d\omega e^{\frac{\omega^3}{3} - x\omega}$$

and C is an infinite contour that consists of two straight line pieces, one that approaches the origin from  $-\infty e^{-i\pi/3}$  at angle  $-\pi/3$  and the other that leaves the origin at angle  $\pi/3$  and goes to  $\infty e^{i\pi/3}$ . The Airy kernel is the case when  $\tau = \sigma$  in (49) and is given by

(51) 
$$\mathcal{A}(\xi,\eta) = \int_0^\infty \operatorname{Ai}(\xi + \lambda) \operatorname{Ai}(\eta + \lambda) d\lambda.$$

Let  $\beta_1 < \cdots < \beta_{L_1}$ ,  $L_1 \ge 1$  be fixed given real numbers. Then the extended Airy kernel gives a determinantal point process on  $L_1$  lines  $\{\beta_1, \ldots, \beta_{L_1}\} \times \mathbb{R}$  defining a point process  $\mu_{A_i}$ , called the extended Airy kernel point process. Let  $A_1, \ldots, A_{L_2}, L_2 \ge 1$  be finite disjoint intervals in  $\mathbb{R}$  and write for  $\omega_{p,q} \in \mathbb{C}$ 

$$\psi(x) = \sum_{p=1}^{L_2} \sum_{q=1}^{L_1} \omega_{p,q} \mathbb{I}_{\{\beta_q\} \times A_p}(x).$$

Then, we have that

(52) 
$$\mathbb{E}\left[\exp\left(\sum_{p=1}^{L_2}\sum_{q=1}^{L_1}w_{p,q}\mu_{\mathrm{Ai}}(\{\beta_q\}\times A_p)\right)\right] = \det\left[\mathbb{I} + (e^{\psi} - 1)\mathcal{A}\right]_{L^2(\{\beta_1,\dots,\beta_{L_2}\}\times\mathbb{R})}$$

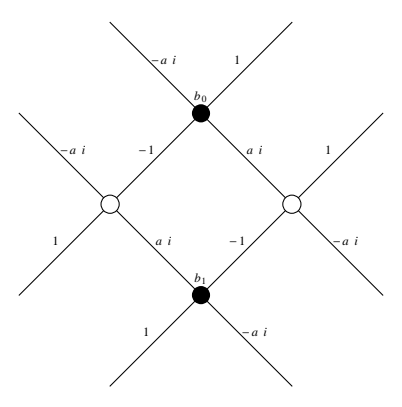
which defines the extended Airy kernel point process

Note that a single line of the extended Airy kernel point process is the Airy kernel point process, that is

(53) 
$$\mathbb{E}\left[\exp\left(\sum_{p=1}^{L_2} w_{p,1} \mu_{\mathrm{Ai}}(\{\beta_1\} \times A_p)\right)\right] = \det\left[\mathbb{I} + (e^{\psi} - 1)\mathcal{A}\right]_{L^2(\{\beta_1\} \times \mathbb{R})}$$

where  $\psi$  is modified accordingly.

Let  $\xi$  denote the Airy kernel point process on  $\mathbb{R}$ . The Airy kernel point process has the property that  $\xi(t,\infty) < \infty$ , that is the number of particles in  $(t,\infty)$  is finite. This means that there is a last particle of the Airy kernel point process, which we denote by  $\xi_{\max}$  and we can find its distribution. By setting  $\phi = \mathbb{I}_{(t,s)}$  in



(17) with s>t, sending  $s\to\infty$  and using the dominated convergence theorem, we get

(54)

$$\mathbb{P}[\xi_{max} < t] = \sum_{n=0}^{\infty} \frac{(-1)^n}{n!} \int_{t}^{\infty} \det \mathcal{A}(x_i, x_j)_{1 \le i, j \le n} d^n \lambda(x) = \det(\mathbb{I} - \mathcal{A})_{L^2((t, \infty))}.$$

The above distribution is the GUE-Tracy Widom distribution [TW94].

We now define the Airy-2 process,  $t \mapsto A(t)$  through its finite dimensional distributions. For any  $s_i \in \mathbb{R}$ , it is the process such that

(55) 
$$\mathbb{P}[A(\beta_1) \le s_1, \dots, A(\beta_m) \le s_m] = \det(\mathbb{I} - L)_{L^2(\{\beta_1, \dots, \beta_{L_0}\} \times \mathbb{R})}$$

where

$$L(\beta_i, \xi_i; \beta_j, \xi_j) = \mathbb{I}_{(s_i, \infty)}(\xi_i) \mathcal{A}(\beta_i, s_i; \beta_j, s_j) \mathbb{I}_{(s_j, \infty)}(\xi_j).$$

Locally, the Airy process has Brownian paths, but is not a Markov process. It appears in a wide number of settings such as in KPZ Universality and governing the fluctuations of interface models. Indeed, the Airy process governs the fluctuations of the frozen-rough boundary for domino tilings of the Aztec diamond [Joh05] and universality has only recently been achieved for lozenge tilings with arbitrary boundary conditions [AG21].

3.3. A saddle point analysis. In these lecture notes, we give an example of using the inverse Kasteleyn matrix for the Aztec diamond to get both a local limit and an interface fluctuation result. This example illustrates the saddle point analysis technique in a relatively simple setting.

For  $w \in \mathbb{W}_n^{Az}$  and  $b = (x_1, x_2) \in \mathbb{B}_n^{Az}$ , we choose the Kasteleyn weighting

$$(56) K_n^{\mathrm{Az}}(b,w) = \begin{cases} (-1)^{l+(x_1+x_2-1)/2} & \text{if } w = b+(-1)^l e_1 \in \mathbb{W} \\ (-1)^{l+(x_1+x_2-1)/2} a \text{if } w = b-(-1)^l e_2 \in \mathbb{W} \\ 0 & \text{otherwise.} \end{cases}$$

Then, from [CJY15], we have that for  $x \in W_n^{Az}$  and  $y \in B_n^{Az}$ , we choose the Kasteleyn weighting

(57) 
$$(K_n^{\text{Az}})^{-1}(x,y) = \begin{cases} f_1(x,y) & \text{for } x_1 < y_1 + 1\\ f_1(x,y) - f_2(x,y) & \text{for } x_1 \ge y_1 + 1 \end{cases}$$

where

(58) 
$$f_1(x,y) = \frac{(-1)^{(y_1+y_2+x_1+x_2)/4}}{(2\pi i)^2} \int_{\mathcal{E}_2} \int_{\mathcal{E}_1} \frac{w^{y_1/2}}{z^{(x_1+1)/2}(w-z)} \frac{(a+z)^{x_2/2}(az-1)^{(2n-x_2)/2}}{(aw-1)^{(2n+1-y_2)/2}(a+w)^{(y_2+1)/2}} dz dw$$

and

$$f_2(x,y) = \frac{(-1)^{(x_1+x_2+y_1+y_2)/4}}{2\pi i} a^{(y_2-x_2-1)/2} \int_{\mathcal{E}_1} \frac{z^{(y_2-x_2-1)/2} (1/a+z)^{(y_1-x_1-1)/2}}{(1/a+a+z)^{(y_2-x_2+1)/2}} dz$$

where  $\mathcal{E}_1$  is the positively oriented contour  $|z| = \varepsilon$ ,  $\mathcal{E}_2$  is the positively oriented contour  $|w - 1/a| = \varepsilon$  and the contours do not intersect.

We will work with the following correlation kernel whose proof is an exercise.

**Lemma 3.1.** Consider the point process of the dimers of the form ((2s, 2r + 1), (2s - 1, 2r)) for  $s \in \{1, ..., n\}$  and r is fixed. Then, these dimers form a determinantal point process whose correlation kernel is given by

(60) 
$$L(x_1, x_2) := -\frac{1}{(2\pi i)^2} \int_{\mathcal{E}_1} dz \int_{\mathcal{E}_2} dw \frac{w^{x_2}}{z^{x_1}} \frac{(a+z)^r (az-1)^{n-r}}{(aw-1)^{n-r} (a+w)^{r+1} (w-z)}$$

For the rest of the lecture, we will set a=1, n to be divisible by 4 and  $r=\frac{3n}{4}$ . Let

(61) 
$$z_c = z_c(\alpha) = \frac{1 + \sqrt{1 - 16\alpha + 16\alpha^2}}{4(1 - \alpha)}$$

for  $\alpha_l \leq \alpha \leq \alpha_r$  where

(62) 
$$\alpha_l = \frac{1}{4}(2 - \sqrt{3}) \text{ and } \alpha_r = \frac{1}{4}(2 + \sqrt{3})$$

Introduce the function

(63) 
$$g(z) = \frac{3}{4}\log(1+z) + \frac{1}{4}\log(z-1) - \alpha\log z.$$

which has critical points  $z_c$  and  $\overline{z_c}$  for  $\alpha_l < \alpha < \alpha_r$  and a double critical point at  $z_c$  when  $\alpha = \alpha_l$  or  $\alpha_r$ . We have the following lemmas on the asymptotics of the kernels.

**Lemma 3.2.** For  $i \in \{1, 2\}$ , set  $x_i = \alpha n + X_i$  where  $X_i \in \mathbb{Z}$  is fixed with n and  $\alpha_l < \alpha < \alpha_r$  so that  $z_c \in \mathbb{H}_+$ . Then, uniformly on compact sets, we have

(64) 
$$L(\alpha n + X_1, \alpha n + X_2) = \frac{1}{2\pi i} \int_{\overline{z_c}}^{z_c} dz \frac{z^{X_2 - X_1}}{z + 1} + O(n^{-\frac{1}{2}})$$

**Lemma 3.3.** For  $i \in \{1,2\}$ , set  $x_i = \alpha_l n + \lambda \xi_i n^{\frac{1}{3}}$  where  $\xi_i \in \mathbb{R}$  is fixed in some compact set, where  $\lambda = z_c(\alpha_l)(-g'''(z_c(\alpha_l))/2)^{1/3}$ . Then, uniformly for  $\xi, \eta$  on a compact subset of  $\mathbb{R}$ , we have

(65) 
$$\lim_{n \to \infty} \lambda n^{1/3} z_c(\alpha_l)^{\xi_1 - \xi_2} L(\alpha_l n + \lambda n^{\frac{1}{3}} \xi_1, \alpha_l n + \lambda n^{\frac{1}{3}} \xi_2) = \frac{1}{z_c(\alpha_l) + 1} \mathcal{A}(\xi_1, \xi_2).$$

We only give sketch proofs of the above two results with the main focus on the second result. The first result is a local limit and is related to the Gibbs measure in [KOS06] introduced earlier in the lecture. This can be seen by evaluating the Gibbs measure for this model and a change of variables. For the second result, notice that there is a coefficient in front of the Airy kernel term. This corresponds to an independent thinning of the Airy kernel point process. Indeed, let  $\{x_j\}$  be the points of a determinantal point process with correlation kernel K and let  $\{n_j\}$  be an independent thinning with  $\mathbb{P}[n_j = 1] = \alpha$  and let  $\phi = 1 - e^{-\psi}$ . Then, by denoting  $\mathbb{E}_n$  and  $\mathbb{E}_K$  to be the expectation with respect to the thinning and determinantal point processes respectively, we have that

(66) 
$$\mathbb{E}[e^{-\sum_{j} n_{j} \psi(x_{j})}] = \mathbb{E}_{K} \mathbb{E}_{n}[\prod_{j} (1 - (1 - e^{-n_{j} \psi(x_{j})}))] = \mathbb{E}_{K}[\prod_{j} (1 - \alpha \phi(x_{j}))]$$

which gives a multiplicative factor of  $\alpha$  in front of K in (17) as required. We can do a similar computation for  $\alpha_r$  as given in Lemma 3.3, but the coefficient is greater than 1, which corresponds to a thickening of the Airy kernel point process with a geometric random variable and the resulting point process is no longer simple [CJY15].

Sketch proof of Lemma 3.3. The main steps to prove this result are to

- Express  $L(x_1, x_2)$  in terms of the saddle point function g(z) and identify the critical points of g(z).
- Identify the curves of steepest ascent and descent and deform the contours to the curves of steepest ascent and descent, taking care of additional contributions from crossing contours.
- Split the contours into a local contribution and a global contribution, arguing that the global contribution is negligible when compared to the local contribution.
- Evaluate the local contribution which will give the main contribution.

In the list above, we will omit step 3 and only state the contours of steepest descent and ascent.

From the form of  $L(x_1, x_2)$  given in (60) and the choice of  $x_1$  and  $x_2$  given in the statement of Lemma 3.3, we have that

(67) 
$$L(x_1, x_2) = -\frac{1}{(2\pi i)^2} \int_{\mathcal{E}_1} dz \int_{\mathcal{E}_2} dw \frac{w^{\lambda n^{1/3} \xi_2}}{z^{\lambda n^{1/3} \xi_1}} \frac{1}{(1+w)(w-z)} e^{ng(z)-ng(w)}.$$

For the integration contours we choose the steepest descent contours given by the level lines of the imaginary part of g(z) starting at  $z_c$ . It can be seen that we will have two ascending contours for the real part of g(z) which will leave in the directions  $e^{\pm \pi i/3}$  and go to infinity. We deform the contour  $\mathcal{E}_2$  to a contour  $\Gamma_2$  consisting of these two pieces. We have two descending contours going from  $z_c$  to -a leaving in the directions  $e^{\pm 2\pi i/3}$  and these can be combined into a contour  $\Gamma_1$  and thus we deform  $\mathcal{E}_1$  to this contour  $\Gamma_1$ .

For the local contribution, we make the local change of variables  $z - z_c = c_0 \omega_1 i n^{-1/3}$  and  $w - z_c = c_0 \omega_2 i n^{-1/3}$  where  $c_0$  is a constant to be determined. We have that by a Taylor series (68)

$$ng(z) - \lambda n^{\frac{1}{3}} \xi_1 \log z = ng(z_c) - \lambda n^{\frac{1}{3}} \xi_1 \log z_c - \frac{c_0^3 \omega^3}{3!} ig'''(z_c) - \frac{\lambda \xi_1 c_0 \omega_1 i}{z_c} + O(n^{-\frac{1}{3}}).$$

We can set  $c_0 = (-g'''(z_c)/2)^{1/3}$  and  $\lambda$  as given in the statement of the lemma so that the above equation becomes

(69) 
$$ng(z) - \lambda n^{\frac{1}{3}} \xi_1 \log z = ng(z_c) - \lambda n^{\frac{1}{3}} \xi_1 \log z_c + \frac{i\omega_1^3}{3} - \xi_1 \omega_1 + O(n^{-\frac{1}{3}}).$$

Substituting the above equation back into (67) and doing the same for the w variable gives

(70)

$$\lim_{n \to \infty} -\lambda n^{1/3} z_c^{\xi_1 - \xi_2} L(x_1, x_2) = \frac{1}{z_c + 1} \frac{1}{(2\pi i)^2} \int_{\Gamma} dz \int_{\Gamma} dw \frac{e^{iz^3/3 + i\xi_1 z + iw^3/3 + i\xi_2 w}}{i(z + w)}$$

where  $\Gamma$  is given by  $z(t) = -te^{(\pi-\theta)i}$ , t < 0 and  $z(t) = te^{i\theta}$ ,  $t \ge 0$ , with a fixed  $0 < \theta < \pi/3$ . The result follows since the integral on the right side is exactly the Airy kernel.

Sketch proof of Lemma 3.2. We evaluate the same steps as given above in the proof of Lemma 3.3, however time the contours cross. The crossing contours give the main contribution. We can evaluate the remaining double integral using the saddle point analysis and we get that this is  $O(n^{-\frac{1}{2}})$ .

The other fluctuation type result around the limit shape is the fluctuations of the height function in the rough region, which is typically given by a Gaussian free field for flat regions [Ken00, Ken01, BLR20] as well as for stepped regions [BF14, Pet15, BG18, BK18, BN25].

## 3.4. Lecture 3 Exercises.

Exercise 16. Prove Lemma 3.1.

Exercise 17. Suppose that  $\{x_j\}$  be the points of a determinantal point process with correlation kernel K and let  $\{n_j\}$  be a geometric random variable with parameter  $\beta$  and let  $\phi = 1 - e^{-\psi}$ . Give a similar form to (66) for  $\mathbb{E}[e^{-\sum_j n_j \psi(x_j)}]$  where  $\phi = 1 - e^{-\psi}$  and  $\sum_j$  is the sum over the particles of the determinantal point process  $\{x_j\}$ .

#### References

- [ADPZ20] K. Astala, E. Duse, I. Prause, and X. Zhong. Dimer models and conformal structures. arXiv preprint arXiv:2004.02599, 2020.
- [AG21] Amol Aggarwal and Vadim Gorin. Gaussian unitary ensemble in random lozenge tilings. arXiv:2106.07589, 2021.
- [Agg23] Amol Aggarwal. Universality for lozenge tiling local statistics. *Annals of Mathematics*, 198(3):905–1041, 2023.
- [BD19] Tomas Berggren and Maurice Duits. Correlation functions for determinantal processes defined by infinite block Toeplitz minors. Adv. Math., 356:106766, 48, 2019.
- [BdT24] Cédric Boutillier and Béatrice de Tilière. Fock's dimer model on the aztec diamond, 2024.
- [BF14] A. Borodin and P.L. Ferrari. Anisotropic Growth of Random Surfaces in 2+1 Dimensions. Comm. Math. Phys., 325:603-684, 2014.
- [BG18] Alexey Bufetov and Vadim Gorin. Fluctuations of particle systems determined by Schur generating functions. Adv. Math., 338:702-781, 2018.
- [BK18] Alexey Bufetov and Alisa Knizel. Asymptotics of random domino tilings of rectangular Aztec diamonds. Ann. Inst. Henri Poincaré Probab. Stat., 54(3):1250–1290, 2018.
- [BL23] Nathanaël Berestycki and Mingchang Liu. Piecewise temperleyan dimers and a multiple SLE8.  $arXiv\ preprint\ arXiv:2301.08513,\ 2023.$

- [BLR20] Nathanaël Berestycki, Benoît Laslier, and Gourab Ray. Dimers and imaginary geometry. *Annals of Probability*, 48(1):1–52, 2020.
- [BN25] Tomas Berggren and Matthew Nicoletti. Gaussian free field and discrete gaussians in periodic dimer models, 2025.
- [BO00] Alexei Borodin and Grigori Olshanski. Distributions on partitions, point processes, and the hypergeometric kernel. *Communications in Mathematical Physics*, 211(2):335–358, 2000.
- [Bor10] A. Borodin. Determinantal point processes. In G. Akemann, J. Baik, and P. Di Francesco, editors, *The Oxford Handbook of Random Matrix Theory, Chapter 11*. Oxford University Press, USA, 2010.
- [CD23] Sunil Chhita and Maurice Duits. On the domino shuffle and matrix refactorizations. Comm. Math. Phys., 401(2):1417–1467, 2023.
- [CJY15] Sunil Chhita, Kurt Johansson, and Benjamin Young. Asymptotic domino statistics in the Aztec diamond. Ann. Appl. Probab., 25(3):1232–1278, 2015.
- [CKP01] H. Cohn, R. Kenyon, and J. Propp. A variational principle for domino tilings. J. Amer. Math. Soc., 14:297–346, 2001.
- [CY14] Sunil Chhita and Benjamin Young. Coupling functions for domino tilings of Aztec diamonds. *Adv. Math.*, 259:173–251, 2014.
- [DK21] Maurice Duits and Arno B. J. Kuijlaars. The two-periodic Aztec diamond and matrix valued orthogonal polynomials. J. Eur. Math. Soc. (JEMS), 23(4):1075–1131, 2021.
- [EKLP92] N. Elkies, G. Kuperberg, M. Larsen, and J. Propp. Alternating-sign matrices and domino tilings I and II. J. Algebraic Combin., 1:111–132, 219–234, 1992.
- [Gor21] Vadim Gorin. Lectures on random lozenge tilings, volume 193 of Cambridge Studies in Advanced Mathematics. Cambridge University Press, Cambridge, 2021.
- [Joh05] K. Johansson. The arctic circle boundary and the Airy process. Ann. Probab., 33:1–30, 2005.
- [Joh06] K. Johansson. Random matrices and determinantal processes. In A. Bovier, F. Dunlop, A. van Enter, F. den Hollander, and J. Dalibard, editors, Mathematical Statistical Physics, Session LXXXIII: Lecture Notes of the Les Houches Summer School 2005, pages 1–56. Elsevier Science, 2006.
- [Joh18] Kurt Johansson. Edge fluctuations of limit shapes. In *Current developments in mathematics 2016*, pages 47–110. Int. Press, Somerville, MA, 2018.
- [Kas61] P. W. Kasteleyn. The statistics of dimers on a lattice: I. The number of dimer arrangements on a quadratic lattice. *Physica*, 27:1209–1225, 1961.
- [Kas63] P.W. Kasteleyn. Dimer statistics and phase transitions. J. Math. Phys., 4:287–293, 1963.
- [Ken97] R. Kenyon. Local statistics of lattice dimers. Ann. Inst. H. Poincaré Probab. Statist., 33(5):591–618, 1997.
- [Ken00] Richard Kenyon. Conformal invariance of domino tiling. *The Annals of Probability*, 28(2):759–795, 2000.
- [Ken01] R. Kenyon. Dominos and Gaussian free field. Ann. Probab., 29:1128–1137, 2001.
- [KO07] R. Kenyon and A. Okounkov. Limit shapes and the complex Burgers equation. Acta Math., 199:263–302, 2007.
- [KOS06] R. Kenyon, A. Okounkov, and S. Sheffield. Dimers and amoebae. Ann. of Math., 163:1019–1056, 2006.
- [KP25] Arno B. J. Kuijlaars and Mateusz Piorkowski. Wiener-Hopf factorizations and matrix-valued orthogonal polynomials. *Probab. Math. Phys.*, 6(2):547–580, 2025.
- [KPW00] Richard W. Kenyon, James G. Propp, and David B. Wilson. Trees and matchings. Electron. J. Combin., 7:Research Paper 25, 34, 2000.
- [Kui24] Arno B. J. Kuijlaars. Matrix valued orthogonal polynomials arising from hexagon tilings with 3x3-periodic weightings, 2024.
- [Kuo06] Eric Kuo. Graphical condensation generalizations involving Pfaffians and determinants. arXiv:math/0605154, 2006.
- [Mac75] O. Macchi. The coincidence approach to stochastic point processes. Adv. Appl. Prob., 7:83–122, 1975.

- [MPW63] E. W. Montroll, R. B. Potts, and J. C. Ward. Correlations and spontaneous magnetization of the two-dimensional Ising model. *Journal of Mathematical Physics*, 4:308–322, 1963.
- [Pet15] Leonid Petrov. Asymptotics of uniformly random lozenge tilings of polygons. gaussian free field. *The Annals of Probability*, 43(1):1–43, 2015.
- [Pro03] J. Propp. Generalized Domino-Shuffling. Theoret. Comput. Sci., 303:267–301, 2003.
- [Rus18] Marianna Russkikh. Dimers in piecewise temperleyan domains. Communications in Mathematical Physics, 359(1):189–222, 2018.
- [Sos00] A.B. Soshnikov. Determinantal random point fields. Russian Math. Surveys, 55:923–976, 2000.
- [Tem74] H. N. V. Temperley. Enumeration of graphs on a large periodic lattice. In Combinatorics (Proc. British Combinatorial Conf., Univ. Coll. Wales, Aberystwyth, 1973), volume No. 13 of London Math. Soc. Lecture Note Ser., pages 155–159. Cambridge Univ. Press, London-New York, 1974.
- [TF61] H. N. V. Temperley and M. E. Fisher. Dimer problem in statistical mechanics—an exact result. *Philos. Mag. (8)*, 6:1061–1063, 1961.
- [Thu90] William P. Thurston. Conway's tiling groups. Amer. Math. Monthly, 97(8):757–773, 1990.
- [TW94] C.A. Tracy and H. Widom. Level-spacing distributions and the Airy kernel. Comm. Math. Phys., 159:151–174, 1994.